

A Novel Three-polar Representation for R^3 Surfaces : Performance and Stability for Invariant 3D Faces Description

Majdi Jribi¹ et Faouzi Ghorbel¹

¹CRISTAL Laboratory, GRIFT Research Group
Ecole Nationale des Sciences de l'Informatique
La Manouba University, Tunisia

{majdi.jribi, faouzi.ghorbel}@ensi.rnu.tn

Résumé

We intend here to introduce a new curved surface representation. It is called three-polar since it is constructed by the superposition of the three geodesic potentials generated from three reference points of the surface. By sampling this superposition, invariant points are obtained. The accuracy of the three-polar representation for 3D human faces description is performed in the mean of the Hausdorff distance. A comparison between this representation and the one composed of the level curves around the nose tip is established in the sense of the stability under errors on the nose tip positions.

Mots clefs

Three-polar, geodesic, 3D, potential, superposition, level set, face, curve, Hausdorff, stability.

1 Introduction

In the recent years, there has been a growing development of the 3D technologies. Thus, 3D shape analysis and description has received a great deal of attention over these last few years. Actually, R^3 surfaces description becomes a necessary task for pattern recognition, computer vision and 3D movement analysis. In practice, the data obtained from 3D sensors is not organized or partially organized like the 3D triangular mesh known as the conventional 3D discrete surface representation. Therefore, one of the major issues faced today in the three dimensional imaging field is the construction of a surface representation that ensures several properties. The invariance under some transformations and different parametrisations, the independence from the point of view and the robustness to some local variations in shape consist the most important ones. In the literature, the three dimensional surface description methods can be classified into four major categories : the transform based approaches, the 2D views, the graph ones and those based on statistical features.

For the transform based approaches, after the conver-

sion of the surface onto 3D voxels or a spherical grid, specific transformations are applied. The most known ones are 3D Fourier [1], the 3D Radon [2], the angular radial transform [3], the rotation-invariant spherical harmonics [4], the uniformization [5] and the spherical wavelet descriptors [6].

In the two dimensional view based methods, a collection of 2D projections from canonical viewpoints is realized. Then, planar image descriptors are computed as Zernike moments [7] and Fourier descriptors [8].

The graph based approaches have the potential to code geometrical and topological shape properties in an intuitive manner. The usually used descriptors are Reeb graphs [9] and the skeletal ones [10].

For the fourth description category, numerical attributes of the 3D object are collected. Several past works adopted this approach for invariant features extraction like the works of high curvature area determination [11], the generalized shape distribution [12] and the extend Gaussian image [13]. Bannour et al. [14] proposed a new surface pseudo-reparametrisation by the extraction of a curves network determined by iso-curvature features computation. Other methods impose the use of local coordinates by the exponential map around a point belonging to the two dimensional manifold obtained by wrapping a neighborhood of this point by the polar coordinates of the tangent plane at the same point or by constructing a set of geodesic circles relative to a given reference point [15, 16, 17]. The stability of these last methods remains dependent on the robustness of the reference point detection. In recent works, Jribi et al. [26] and Ghorbel et al. [25] proposed a new representation that they called a bipolar one. It consists on the superposition of the two geodesic potentials generated from two reference points instead of one reference point. The goal was to provide a more stability to the representations based on only one reference point [15, 16, 17].

We propose in this paper a novel curved surface representation that we qualify by three-polar. It is an attempt to generalize what is known by local coordinates around a reference point. It is constructed from the superposition of the three geodesic potentials generated from three reference points of the surface. The proposed representation is obtained by sampling the sum of these three geodesic potentials. The performance of such representation for 3D human faces' description is proved. A comparison between the proposed representation and the one based on only one reference point (the nose tip) is established in the sense of the stability under errors on the reference points positions.

Thus, this paper will be structured as follows : We present in the second section the mathematical formulation of the three-polar representation. The used similarity metric to compare between shapes is illustrated in the third section. We show in the fourth section the performance of the three-polar representation for 3D faces' description. In the last section, a comparison between the three-polar representation and the unipolar one in the sense of the stability under errors on the nose tip positions is established.

2 Mathematical formulation of the three-polar representation

We consider here a two dimensional differential manifold S and we denote by U_r the geodesic potential generated from a reference point r . For each point p of S , $U_r(p)$ is the length of the geodesic curve joining p to r . For a given real value λ , the points with geodesic potential values equal to λ form a curve that we denote by C_r^λ . It belongs to the surface and is called the geodesic of level λ .

We describe here the construction process of the three-polar representation which is based on the superposition of the three geodesic potentials generated from the three reference points. Thus, let consider $\{r_i, i = 1..3\}$ three points of the two differential manifold S . Let $\{U_{r_i}, i = 1..3\}$ be their corresponding potentials functions. We denote by $U_3 = \sum_{i=1}^3 U_{r_i}$ the geodesic potential constructed by the sum of the three geodesic potentials generated from $\{r_i, i = 1..3\}$.

Let p^* be a point of S . Therefore there exist $\{\lambda_i^*, i = 1..3\}$ such that p^* belongs to the three level curves $\{C_{r_i}^{\lambda_i^*}, i = 1..3\}$. Let $U_3^* = \min\{U_3\}$. The points of the surface with the same geodesic sum are invariant. By considering a levels set of this sum, we construct a system of invariant points under the rotations' group $SO(3)$. The representation that we propose is constructed by varying these levels from 0 to the integer K . This integer represents the maximum value determined by

the interest region extend which lies between the three reference points and its neighborhood on the surface. Therefore, the descriptor can be written as following :

$$M_3^k(S) = \{p^* \in S; U_3(p^*) = U_3^* + \frac{k}{K}(\alpha_K - U_3^*), k = 0..K\} \quad (1)$$

Where α_K is the maximum of the geodesic sum.

3 Similarity metric

It is important to define the used similarity metric to compare between different shapes. The well known Hausdorff shape distance introduced by Ghorbel in [19, 20] is chosen. Following the same process, we denote by G the group representing all possible normalized parametrisations of surfaces which can be the real plane R^2 or the unit sphere S^2 . we consider the space of all surface pieces as the set of all 3D objects assumed diffeomorphic to G which can be assimilated to a subspace of $L_{R^3}^2(G)$ formed by all square integrated maps from G to R^3 . The direct product of the Euler rotations group $SO(3)$ by the group G , acts on such space in the following sense :

$$SO(3) \times G \times L_{R^3}^2(G) \rightarrow L_{R^3}^2(G) \quad (2)$$

$$\{A, (u_0, v_0), S(u, v)\} \rightarrow AS(u + u_0, v + v_0)$$

The 3D Hausdorff distance Δ can be written for every S_1 and S_2 belonging to $L_{R^3}^2(G)$ and g_1 and g_2 to $SO(3)$ as follows :

$$\Delta(S_1, S_2) = \max(\rho(S_1, S_2), \rho(S_2, S_1)) \quad (3)$$

Where :

$$\rho(S_1, S_2) = \sup_{g_1 \in SO(3)} \inf_{g_2 \in SO(3)} \|g_1 S_1 - g_2 S_2\|_{L^2} \quad (4)$$

$\|S\|_{L^2}$ denotes the norm of the functional banach space $L_{R^3}^2(G)$.

Due to the fact that the euclidean rotations preserve this norm, it is easy to show that this distance is reduced to the following quantity :

$$\Delta(S_1, S_2) = \inf_{h \in SO(3)} \|S_1 - h S_2\|_{L^2} \quad (5)$$

After that, we consider a normalized version of Δ so that the variations of this normalized distance are confined to the interval $[0,1]$. We try to achieve the real value of this distance with an adaptative version of the well known Iterative Closest Point (ICP) algorithm [18].

4 Human face description with the three-polar representation

The description and the analysis of three dimensional shapes have become more and more attracting especially with the availability of 3D shape scanners. The 3D face

description has received a great deal of attention over the last few years because of its various application domains. The biometrics are one of the most important applications. We test here the accuracy of the three-polar representation on the 3D meshes of the database Bosphorus [21] in the sense of the Hausdorff distance. We use a total of ten faces that can be grouped into two classes. A first class contains five faces of the same person with different expressions and a second one contains five faces of different persons.

4.1 The choice and the automatic extraction of the reference points

The first step of the three-polar representation construction is the choice of the reference points from the face. There is a general agreement that eyes are the most important facial features [24]. Indeed, they are a crucial source of information about the state of human being. Moreover, their appearance is less variant to certain face changes. Therefore, we choose to use the two outer corners of the eyes as reference points for the proposed three-polar representation. Since the nose tip is commonly used for many facial surfaces' description [15, 16, 17], it will be also chosen as a reference point in the three-polar representation. For the automatic extraction of these points, we refer to the work of Szeptycki et al. [23]. This method is based on a curvatures analysis with the use of a generic face model generated from a set of faces.

4.2 Geodesic potentials computation

Having extracted the reference points, the geodesic distances between any reference points and each vertex of the surface should be computed. This computation must take in consideration the trade off between the the computational cost and the accuracy. We use in the present work a simple method in which the geodesic distance is approximated by Dijkstra's algorithm [22] based on the edges length. This algorithm has a computational cost of order $O(n \log n)$. n is the number of vertices in the mesh.

4.3 Accuracy of the three-polar representation for human face description

After determining the reference points and computing the geodesic distances from these points, the next step consists on the extraction of the levels set of the geodesic sum for the construction of the three-polar representation.

The figure 1 shows the proposed representation with different resolutions which are linked to the number of levels in the representation construction.

To illustrate the effectiveness of the joint introduction in this context of the two notions : the three-polar representation and the Hausdorff distance, the matrix representing the pairwise normalized distances between the ten faces is computed. The first five faces correspond to the first class. The rest belongs to the second class. The

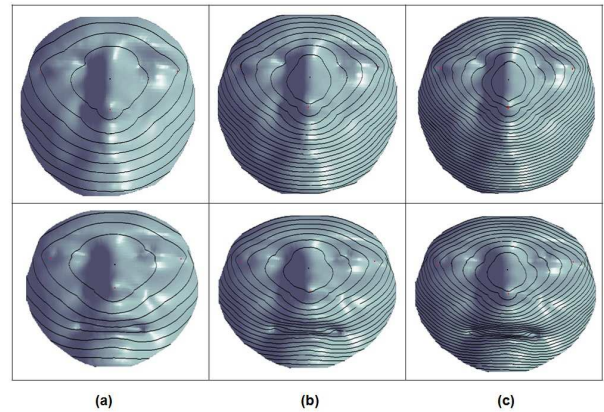


Figure 1 – Row 1 : A neutral face. Row 2 : A face with a surprise expression. (a) The three-polar representation with 9 levels. (b) The three-polar representation with 19 levels. (c) The three-polar representation with 29 levels.

figure 2 illustrates this matrix.

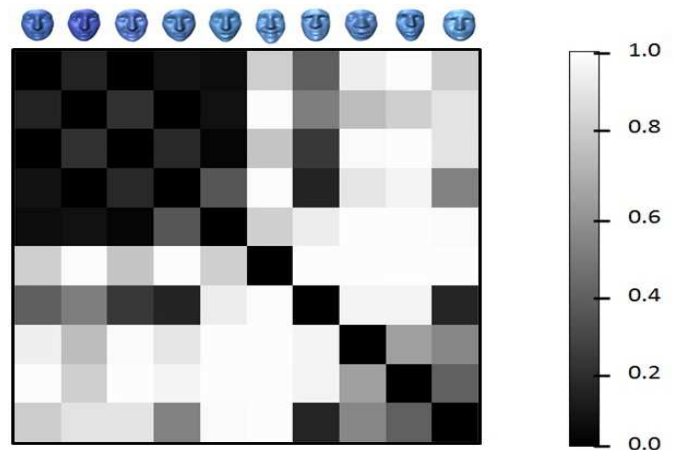


Figure 2 – Matrix of pairwise normalized Hausdorff distances between the ten facial surfaces. The first five faces correspond to the same person while others belong to different individuals

This matrix shows that the distances between the faces of the same persons are smaller compared with the ones computed between faces of different individuals.

5 Stability under errors on reference points positions

We propose to make here a comparison between the three-polar representation and the unipolar one based on only one reference point which corresponds to the nose tip. This comparison will be performed in the sense of the stability under error on their common reference point (the nose tip) positions.

To evaluate this stability, we assume that the nose tip is moved by some geodesic distance around the same point without errors of extraction. The figure 3 illustrates the unipolar representation in two cases : a good extraction of the nose tip (a), and with error of extraction (b).

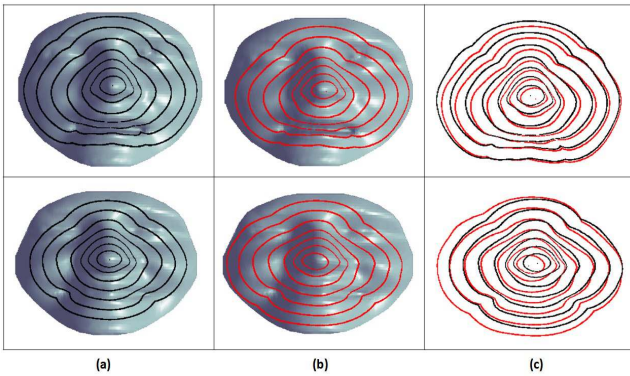


Figure 3 – Row 1 : A face with a surprise expression. Row 2 : A face with a happiness expression (a) The unipolar representation with a good extraction of the nose tip. (b) The unipolar representation with errors on the nose tip positions. (c) : The superposition of the two representations (with and without errors).

The figure 4 shows the three-polar representation for the same two cases with the same errors of the nose tip extraction.

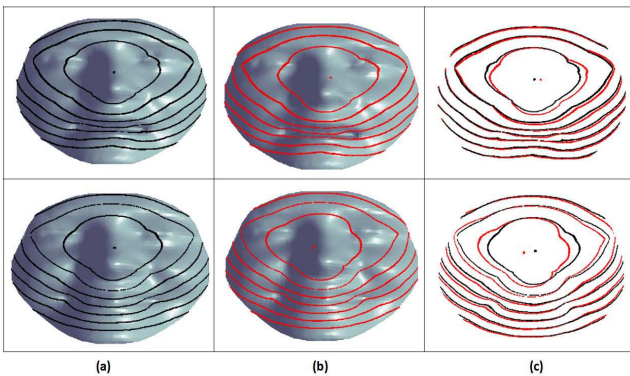


Figure 4 – Row 1 : A face with a surprise expression. Row 2 : A face with a happiness expression. (a) The three-polar representation with a good extraction of the nose tip. (b) The three-polar representation with errors on the nose tip positions. (c) : The superposition of the two representations (with and without errors).

The superposition of the two representations (with and without errors of the nose tip extraction) is illustrated in the figure 5 for the three-polar representation and the

unipolar one.

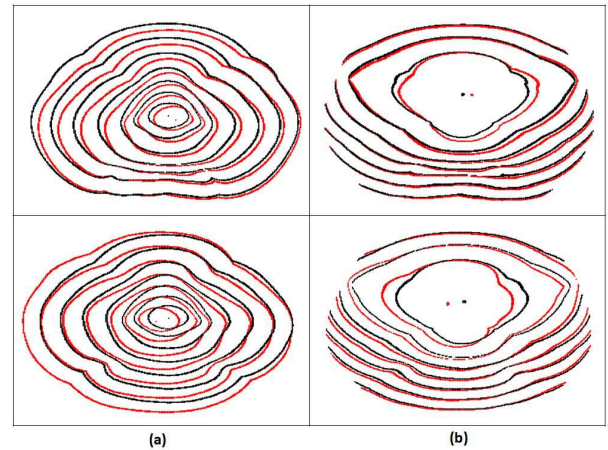


Figure 5 – Row 1 : A face with a surprise expression. Row 2 : A face with a happiness expression. (a) The superposition of the unipolar representations (with and without errors of the nose tip extraction). (b) The superposition of the three-polar representations (with and without errors of the nose tip extraction).

This figure tends to prove that the three-polar representation is more stable than the unipolar one under errors on the nose tip positions. Indeed, for the three-polar representation, there is a better superposition of the level curves (with and without errors of extraction of the nose tip) than the unipolar one.

In the worst cases of extraction errors of the nose tip, we assume that the positions of this point belong to a geodesic level curve having a geodesic radius value equal to R_{Gmax} around the nose tip. The figure 6 illustrates the extremal geodesic level curve of extraction errors.

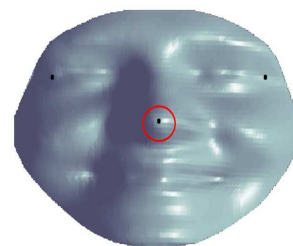


Figure 6 – The extremal geodesic level curve of variation of the nose tip positions with errors of extraction

For the both representations, (three-polar and unipolar), we compute the Hausdorff shape distances between these representations with a good extraction of the nose tip (reference representations) and the ones constructed by varying the positions of the same point along the geodesic level

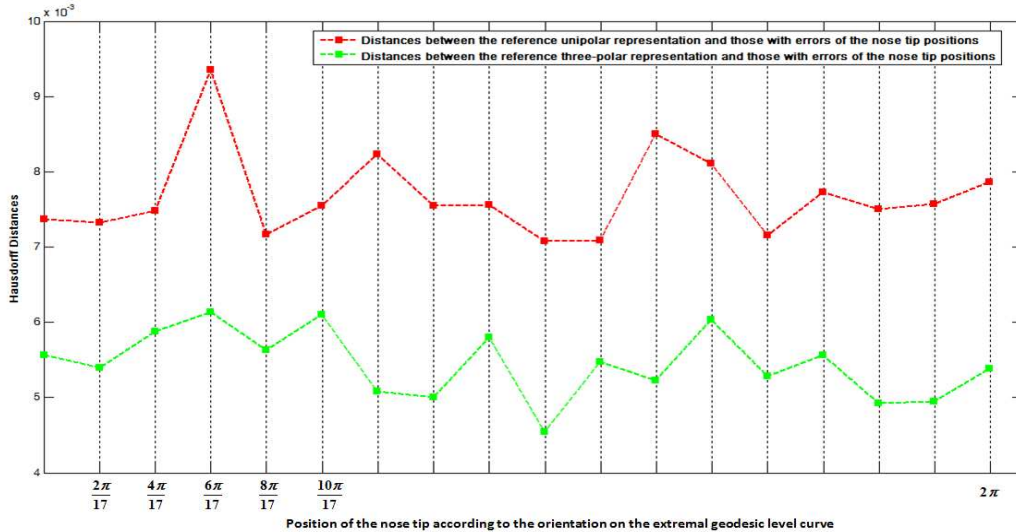


Figure 7 – Evolution of the Hausdorff distances according to the positions of the nose tip with errors of extraction (unipolar representation and three-polar representation)

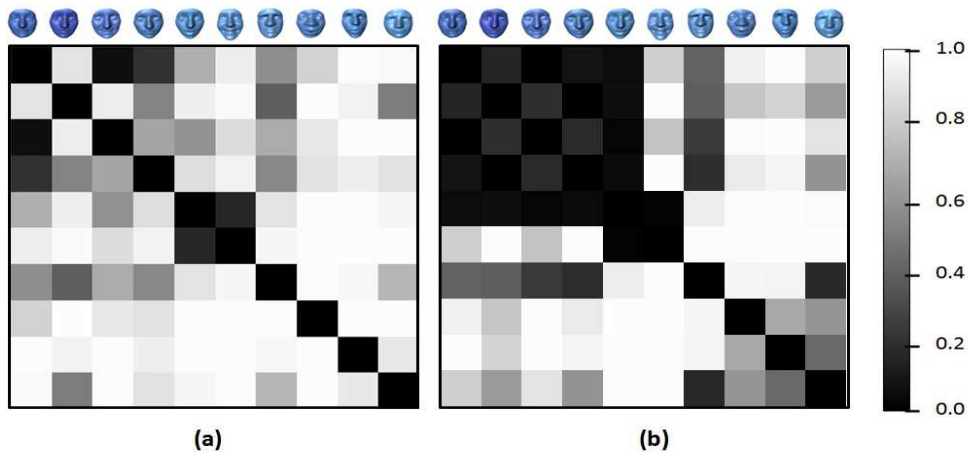


Figure 8 – Matrices of pairwise normalized distances between the ten faces with errors on the nose tip position. (a) : The unipolar representation. (b) : The three-polar representation.

curve of radius value $R_{G_{max}}$. The figure 7 shows these variations according to the orientation of the position of the nose tip on the extremal level curve in the case of extraction errors. The origin of orientation is the same for all the representations. From the observation of figure 7, we can note that the three-polar representation has ensured more stability than the unipolar one.

In order to more illustrate this stability under the natural distortions of the nose tip positions, this point is chosen randomly in a small neighborhood around the same point without errors. The matrices representing the pairwise normalized distance are computed for the two representations. The figure 8 illustrates these matrices. From the comparison of these two matrices, we can note that the three-polar representation is more robust in the sense of stability than

the unipolar representation under errors of the nose tip positions.

6 Conclusion

We have proposed in this paper a novel curved surface representation. It is called a three-polar one since it consists on the superposition of the three geodesic potentials generated from three reference points of the surface. By sampling this continuous representation, a levels set of this superposition is computed. The accuracy of this representation for human face description is proved. Its stability under errors on one reference point positions is established.

We intend in future works to perform the experimentation on a larger number of faces. We propose also to determine of the optimal number of the level curves of the pro-

posed representation.

Références

- [1] V. Burdin, F. Ghorbel, J.D.B.D.L. Tognaye and C. Roux, A three-dimensional primitive extraction of long bones obtained from bi-dimensional Fourier descriptors, *Pattern Recognition Letters*, vol. 13, No 3, 1992, pp. 213-217.
- [2] P. Daras, D. Zarpalas, D. Tzovaras and M.G. Strintzis, Shape Matching Using the 3D Radon Transform, *Second International Symposium 3D Data Processing, Visualization, and Transmission*, 2004, pp. 953-960.
- [3] J. Ricard, D. Coeurjolly and A. Baskurt, Generalizations of Angular Radial Transform for 2D and 3D Shape Retrieval, *Pattern Recognition Letters*, vol. 26, No 14, 2005, pp. 2174-2186.
- [4] M. Kazhdan, T. Funkhouser and S. Rusinkiewicz, Rotation Invariant Spherical Harmonic Representation of 3D Shape Descriptors, *Eurographics/ACM SIGGRAPH Symposium on Geometry Processing*, 2003, pp. 156-164.
- [5] W. Bel Hadj Khelifa, A. Ben Abdallah and F. Ghorbel, Three dimensional modeling of the left ventricle of the heart using spherical harmonic analysis, *5th IEEE International Symposium on Biomedical Imaging : From Nano to Macro (ISBI 2008)*, Paris, France, 2008.
- [6] H. Laga, H. Takahashi and M. Nakajima, Spherical Wavelet Descriptors for Content-Based 3D Model Retrieval, *IEEE International Conference on Shape Modeling and Applications*, 2006, pp. 15-25.
- [7] D.Y. Chen, X.P. Tian, Y.T. Shen and M. Ouhyoung, On Visual Similarity Based 3D Model Retrieval, *Computer Graphics Forum*, vol. 22, No 3, 2003, pp. 223-232.
- [8] D.V. Vranic, 3D Model Retrieval. PhD dissertation, *University Of Leipzig*, 2004.
- [9] T. Tung and F. Schmitt, The Augmented Multiresolution Reeb Graph Approach for Content-Based Retrieval of 3D Shapes, *International Journal of Shape Modeling*, vol. 11, No 1, 2005, pp. 91-120, .
- [10] H. Sundar, D. Silver, N. Gagvani and S. Dickinson, Skeleton based Shape Matching and Retrieval, *Shape Modeling International 2003*, 2003, p. 130.
- [11] O.D. Faugeras and M. Hebert, The representation, recognition and positioning of 3D shapes from range data, techniques for 3D machine perception, *Edition A, Rosenfield*, Hollande, 1986.
- [12] Y. Liu, H. Zha and H. Qin, The Generalized Shape Distributions for Shape Matching and Analysis, *IEEE International Conference of Shape Modeling and Applications*, 2006, p. 16.
- [13] S.B. Kang and K. Ikeuchi, The Complex EGI : A New Representation for 3D Pose Determination, *IEEE Transactions on Pattern Analysis and Machine Intelligence*, vol. 15, No 7, 1993, pp. 707-721.
- [14] M.T. Bannour and F. Ghorbel, Isotropie de la représentation des surfaces ; Application à la description et la visualisation d'objets 3D, *RFIA 2000*, 2000, pp. 275-282.
- [15] C. Samir, A. Srivastava and M. Daoudi, Three dimensional face recognition using shapes of facial curves , *IEEE Transactions on Pattern Analysis and Machine Intelligence*, vol. 28, No 11, 2006, pp. 1858-1863.
- [16] A. Srivastava, C. Samir, S.H. Joshi and M. Daoudi, Elastic shape models for face analysis using curvilinear coordinates, *Journal of Mathematical Imaging and Vision*, vol. 33, No 2, 2008, pp. 253-265.
- [17] W. Gadacha and F. Ghorbel, A new 3D surface registration approach depending on a suited resolution : Application to 3D faces, *IEEE Mediterranean and Electrotechnical Conference (MELECON)*, Hammamet, Tunisia, 2012.
- [18] P.J. Besl and N.D. McKay, A method for registration of 3-D shapes, *IEEE Transactions on Pattern Analysis and Machine Intelligence*, vol. 14, No 2, 1992, pp. 239-256.
- [19] F. Ghorbel, A unitary formulation for invariant image description : application to image coding, *special issue Annales des telecommunications*, vol. 53, No 5-6, 1998, pp. 242-260.
- [20] F. Ghorbel, Invariants for shapes and movement. Eleven cases from 1D to 4D and from euclidean to projectives (French version), *Arts-pi Edition*, Tunisia, 2012.
- [21] A. Savran, A. Alyz, H. Dibeklioglu, O. Eliktutan, B. Gkberk, B. Sankur and L. Akarun, Bosphorus Database for 3D Face Analysis, *The First COST 2101 Workshop on Biometrics and Identity Management (BIOID2008)*, 2008.
- [22] E.W. Dijkstra, A note on two problems in connection with graphs, *Numerische Mathematik*, 1959.
- [23] P. Szeptycki, M. Ardabilian and L. Chen, A coarse-to-fine curvature analysis-based rotation invariant 3D face landmarking, *IEEE 3rd International Conference on Biometrics : Theory, Applications, and Systems, 2009. BTAS '09*, 2009.
- [24] P. Campadelli, R. Lanzarotti and G. Lipori, Automatic Facial Feature Extraction for Face Recognition, *Kresimir Delac and Mislav Grgic (Ed.), ISBN : 978-3-902613-03-5, I-Tech*, 2007.
- [25] F. Ghorbel and M. Jribi : A robust invariant bipolar representation for R^3 surfaces : applied to the face description, *Springer, Annals of telecommunications*, vol. 68, No 3-4, 2013, pp. 219-230.
- [26] M. Jribi and F. Ghorbel : Un ensemble d'invariants bipolaires pour les surfaces de R^3 : Application à la description du visage par une approche 3D, *Traitement du signal (TS)*, vol. 29, No 1-2, 2012, pp. 51-63.